JMBFS
Journal of Microbiology, Biotechnology and Food Sciences
International peer-reviewed scientific online journal
Published by Faculty of Biotechnology and Food Sciences

MOLECULAR MODELING AND *IN SILICO* ANALYSIS OF THE MOLYBDATE/TUNGSTATE TRANSPORTER WtpB IN THE HYPERTHERMOPHILIC ARCHAEON *Thermococcus kodakarensis*

Muhammad Tausif Chaudhry, Raheela Chaudhry*

Address(es):
National Metrology Institute of Pakistan (NMIP), Islamabad, Pakistan.

*Corresponding author: tausif_chaudhry@yahoo.com

https://doi.org/10.55251/jmbfs.13078

ARTICLE INFO

Received 18. 7. 2025
Revised 17. 4. 2026
Accepted 29. 4. 2026
Published 1. 6. 2026

Regular article

OPEN ACCESS

ABSTRACT

The WtpB permease from *Thermococcus kodakarensis* KOD1 is a membrane-integrated component of the WtpABC ATP-binding cassette (ABC) transporter system, mediating high-affinity uptake of tungstate (WO_4^{2-}) and molybdate (MoO_4^{2-}), essential metal oxoanions in hyperthermophilic archaea. Using comprehensive *in silico* approaches, we modeled the secondary and tertiary structure of WtpB, revealing nine α-helices with distinct functional domains, including putative periplasmic binding protein (PBP) interaction loops, a conserved gate region, dimer interface, and ABC-ATPase interaction site. Sequence alignment of 31 *Thermococcus* species demonstrated 44.5 % residue conservation, indicating evolutionary stability. Physicochemical profiling showed a high aliphatic index (131.94), isoelectric point of 9.69, and GRAVY score of 0.854, consistent with a thermally stable, hydrophobic transmembrane protein. Structural validation via Ramachandran plot indicated 95.5 % residues in favored regions, while ProQ and QMEAN scores (LG: 9.228; MaxSub: 0.407; QMEAN: 0.549) confirmed model accuracy. Interaction network analysis identified strong associations with WtpA and WtpC (confidence scores >0.99), predicting complex formation. Phylogenetic analysis resolved six clusters within *Thermococcus*, with WtpB sequence identities ranging from 72.6 % (*Pyrococcus furiosus*) to 97.1 % (closely related species), reflecting functional divergence aligned with ecological niches. This integrated structural and evolutionary characterization of WtpB advances understanding of archaeal metal oxoanion transport mechanisms, crucial for maintaining redox metabolism under extreme conditions, and provides a molecular basis for future functional and applied studies targeting hyperthermophilic ABC transport systems.

Keywords: *Thermococcus kodakarensis*; conserved motifs; *in silico* analysis; molebdate/tungstate transporter; WtpB; phylogenetic analysis; tertiary structure prediction

INTRODUCTION

Members of the genus *Thermococcus* are sulfur-reducing, obligately anaerobic hyperthermophilic archaea inhabiting extreme geothermal environments (**Krupovic *et al*., 2013**; **Hetzer *et al*., 2007**), reflecting remarkable ecological and evolutionary adaptability. Among them, *Thermococcus kodakarensis* KOD1 is a key model archaeon with a fully sequenced genome (**Fukui *et al*., 2005**) and a highly thermostable and efficient DNA polymerase (**Nishioka *et al*., 2001**), underscoring its importance in archaeal biology and biotechnology. Hyperthermophilic archaea sustain metabolism under extreme conditions through precise regulation of metal ions, supporting vital cellular function and physiological integrity (**Moustakas, 2021**) where metal oxoanions such as tungstate (WO_4^{2-}) and molybdate (MoO_4^{2-}) play a pivotal role in redox metabolism and enzymatic function (**Mendel and Kruse, 2012; Winiarska *et al*., 2023**). Their selective use reflects an evolutionary adaptation that enhances enzymatic function and stability in some of Earth's most inhospitable habitats.

In *Pyrococcus furiosus*, high-affinity uptake of WO_4^{2-} and MoO_4^{2-} is mediated by the WtpABC transporter, comprising the periplasmic binding protein WtpA, the membrane permease WtpB, and the ATPase WtpC, with a marked preference for tungstate over molybdate (**Bevers *et al*., 2006**). In *Metallosphaera sedula*, only WtpA and WtpC homologues facilitate such transport (**Wheaton *et al*., 2016**). By contrast, sulfate-reducing bacteria such as *Desulfovibrio vulgaris* employ the ModABC system, regulated by the molybdate-responsive transcription factor ModE (**Kazakov *et al*., 2013**). Lacking ModE, hyperthermophilic archaea employ alternative strategies for metal ion homeostasis. The permease WtpB is of particular interest, which constitutes the membrane-integrated component of the WtpABC ATP-binding cassette (ABC) transporter system. Structurally, WtpB is predicted to contain multiple transmembrane α-helices, forming a channel to translocate oxyanions from the periplasm into the cytoplasm (**Bevers *et al*., 2006**). Despite its central role, structural elucidation of WtpB at atomic resolution remains lacking, and its precise transport mechanism in extremophilic contexts requires further investigation.

To address this knowledge gap, a comprehensive structural and evolutionary analysis of WtpB from *T. kodakarensis* KOD1 was carried out. This study presents homology-based models of the two- and three-dimensional structures of the WtpB permease from *T. kodakarensis* KOD1, alongside a comprehensive *in silico* characterization. Structural integrity and model quality were assessed using Ramachandran plot analysis and neural network-based validation tools. Conserved residues and characteristic sequence motifs were identified, and key physicochemical properties were predicted directly from the primary sequence. Additional structural features, including intrinsic disorder, foldability, and bonding patterns, were predicted. Evolutionary relationships were examined through phylogenetic reconstruction and distance analysis across 31 Thermococcus species, providing insights into the conservation and divergence of WtpB within this archaeal lineage.

MATERIAL AND METHODS

Sequence analysis and alignments

The protein sequence of WtpB (accession no. WP_011248973) was obtained from the complete genome sequence of *T. kodakarensis* KOD1 (GenBank accession no. AP006878). Homologous sequences were identified using BLASTP (**Altschul *et al*., 1997**) against the NCBI protein database. WtpB homologs from 30 additional *Thermococcus* species were also retrieved. Functional domains and conserved regions were annotated using the NCBI Conserved Domain Database (CDD; **Wang *et al*., 2023**). Pairwise and multiple sequence alignments were performed with CLUSTAL X v2.1 (**Larkin *et al*., 2007**), and sequence identities were calculated using BioEdit v7.7 (**Hall, 1999**).

Secondary and tertiary structural modeling

Secondary structure prediction of WtpB was performed using JPred4 (**Drozdetskiy *et al.*, 2015**), which indicated a defined arrangement of α-helices and β-sheets. Tertiary structure modeling was conducted via the 3DPro tool on the SCRATCH protein prediction server (**Cheng *et al*., 2005**). The 3DPro tool on the SCRATCH protein prediction server is primarily an ab initio (*de novo*) predictor, which predicts tertiary structures by combining predicted structural features including secondary structure, solvent accessibility, and residue contacts with energy terms derived from PDB statistics and a fragment library with moderate reliability. Final three-dimensional models were visualized using VMD v1.9.3 (**Hsin *et al*., 2008**).

Physicochemical profiling and structural analysis

Key physicochemical parameters—including molecular weight, isoelectric point (pI), molar extinction coefficient at 280 nm, instability index, aliphatic index, and the grand average of hydropathicity (GRAVY)—were calculated using ProtParam (**Gasteiger *et al*., 2003**). Structural features such as disordered residues, disorder probability, domain architecture, and disulfide bond presence were analyzed using the SCRATCH suite (**Cheng *et al*., 2005**). Protein unfoldability was assessed with FoldIndex (**Prilusky *et al*., 2005**), while mean hydrogen bond energy and packing defect percentage were evaluated using VADAR v1.8 (**Willard *et al*., 2003**). The quality of the NMR-derived protein structure was evaluated using ResProx (**Berjanskii *et al*., 2012**), which estimates an equivalent X-ray resolution based on structural features derived from the atomic coordinates.

Structure validation

Structural validation was performed using the Ramachandran plot, a widely accepted metric for assessing protein model quality in the absence of experimental data (**Hollingsworth and Karplus, 2010**). Torsion angle distributions were evaluated using PROCHECK **(Laskowski *et al*., 1993)**, which assesses stereochemical integrity and highlights residues in disallowed regions. In parallel, model quality was further assessed using ProQ, a neural network–based predictor (**Wallner and Elofsson, 2003**), and QMEAN, which provides a composite quality score for model ranking relative to experimentally derived structures (**Benkert *et al*., 2009**). MolProbity (**Williams *et al*., 2018**) was used to identify and score conformational outliers in the protein backbone and side chains.

Prediction of WtpB-associated proteins

WtpB protein sequences from 31 *Thermococcus* species were retrieved from the NCBI protein database (www.ncbi.nlm.nih.gov/protein). Functional interaction networks and confidence scores for predicted protein–protein associations were inferred using STRING v12.0 **(Szklarczyk *et al*., 2023**).

Phylogenetic analysis

The evolutionary history was inferred using the neighbor-joining method of **Saito and Nei (1987)** based on 1000 replications. The evolutionary distances among WtpB from 31 *Thermococcus* species including *T. kodakarensis* KOD1 were computed using the number of differences method (**Nie and Kumar, 2000**) with the units of the number of amino acid substitutions per site. The analytical procedure encompassed 32 amino acid sequences. The pairwise deletion option was applied to all ambiguous positions for each sequence pair resulting in a final data set comprising 260 positions. Evolutionary analyses were conducted in MEGA12 (**Kumar *et al*., 2024**).

RESULTS AND DISCUSSION

A comprehensive *in silico* investigation was carried out to define the structural organization, sequence conservation, and evolutionary relationships of WtpB, the membrane-associated permease of the WtpABC transporter system in *T. kodakarensis* KOD1. This analysis integrated secondary and tertiary structure prediction, domain annotation, physicochemical profiling, structural validation, and phylogenetic comparison across 31 *Thermococcus* species, providing detailed insights into the functional architecture and evolutionary conservation of this key transport protein.

Structural features and sequence conservation of WtpB

As predicted by JPred4 (**Drozdetskiy *et al.*, 2015**), WtpB from *T. kodakarensis* KOD1 comprises nine α-helices and two very short β–sheets (Fig. 1). The longest α-helix, helix 7, comprises 33 amino acids, whereas helices 6 and 9 contain only 9 residues each. Of the five loops connecting the helices, three are predicted to be extracellular and two cytoplasmic. Sequence alignment of WtpB orthologs from 31 *Thermococcus* species revealed a high degree of conservation, with 110 out of 247 residues (44.5 %) invariant across all sequences.

Predicted tertiary structure and functional elements of WtpB

A three-dimensional structure of WtpB from *T. kodakarensis* KOD1 is shown in Figure 2. The overall structure of WtpB consisted of nine α-helices. Both the N- and C-termini are cytoplasmic. WtpB comprises four functional elements, as indicated in Fig. 1. In Fig. 3, the three-dimensional model of WtpB is shown in dot representation, with the functional elements highlighted in yellow surface rendering. The conserved C-terminal region WtpB proteins, identified as *VARTLG-X_9-I/V-X-LP* (**Bevers *et al*., 2006**) was located in WtbB as *VARTLG-X_9-I-X-LP*. This conserved sequence is recognition site for the C component of the ABC transporters (**Mourez *et al*., 1997**).

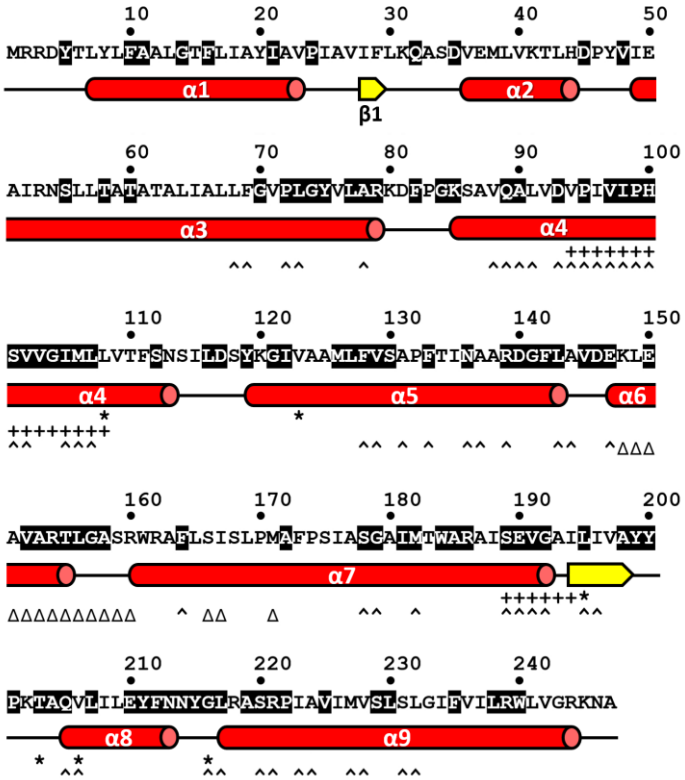

Figure 1 Predicted α-helix and β–sheets distribution in the secondary structure of WtpB from *T. kodakarensis* KOD1. Secondary structure prediction was performed using JPred4. Conserved residues across 31 *Thermococcus* species are indicated in black. Functional regions are annotated as follows: asterisks, putative PBP-binding loops (6 residues); plus signs, conserved gate region (21 residues); carets, dimer interface (54 residues); triangles, ABC-ATPase subunit interface (16 residues).

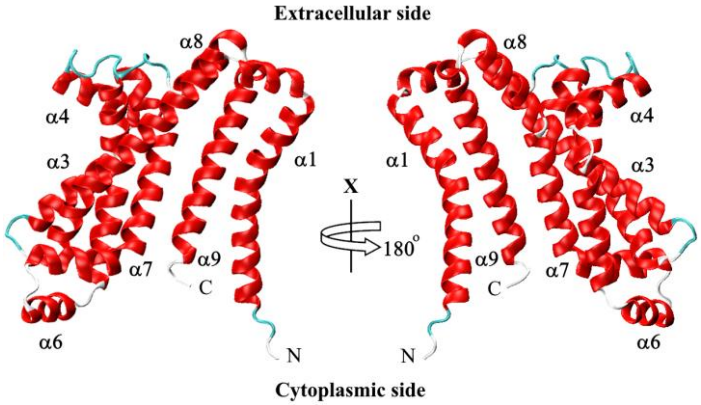

Figure 2 Predicted three-dimensional structure of WtpB from *T. kodakarensis* KOD1, shown before (right) and after (left) a 180° rotation along the x-axis. α-helices are colored red, with turns and loops depicted in cyan and white, respectively. The C- and N-terminals are labeled as C and N. The structure was visualized using VMD 1.9.

The PBP-binding loops of WtpB mediate selective interaction with the periplasmic binding protein, enabling efficient substrate transfer. This coordination links metal oxyanion delivery to ATP hydrolysis. This mechanism underpins the high-affinity and selective uptake of molybdate and tungstate in *T. kodakarensis* and related archaea, as conserved across structurally and functionally similar ABC transporters (**Gerber *et al*., 2008; Bevers *et al*., 2011**). The conserved gate region of WtpB regulates substrate access to the translocation pathway. Upon binding of the PBP to its substrate, conformational changes in WtpB open the gate, enabling precise transfer of metal oxyanions and ensuring high-affinity, specific uptake of molybdate and tungstate. The dimer interface stabilizes the arrangement of two WtpB subunits and enables conformational changes that couple ATP hydrolysis to substrate translocation. This coordination ensures efficient and directional uptake of molybdate and tungstate. The ABC-ATPase interface of WtpB transmits conformational changes from ATP hydrolysis to the transmembrane domain, driving molybdate and tungstate transport. This coupling ensures energy-dependent, directional substrate uptake.

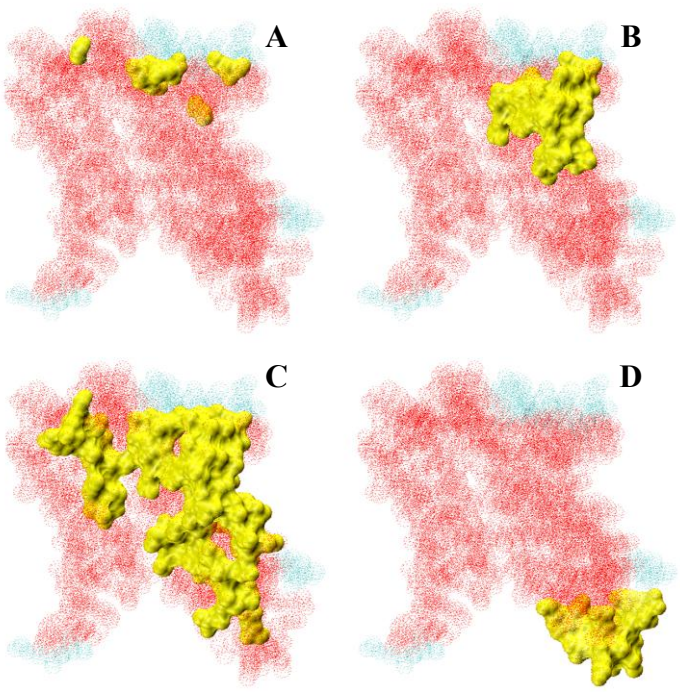

Figure 3 Predicted functional elements of WtpB from *T. kodakarensis* KOD1. The predicted structure of WtpB is shown in a dot representation, with functional elements highlighted as yellow surface features. (A) putative PBP-binding loops, (B) conserved gate region, (C) dimer interface, (D) ABC-ATPase subunit interface.

Physiochemical characterization

The physicochemical properties of WtpB from *T. kodakarensis* KOD1, as predicted by ProtParam, are summarised in Table 1. The isoelectric point (pI) was calculated to be 9.69, at which the net charge of the protein is zero. The instability index, a predictor of *in vitro* protein stability **(Guruprasad *et al.*, 1990)**, was 27.52, suggesting that WtpB is stable under standard laboratory conditions, as values below 40 are generally indicative of stability. The aliphatic index **(Ikai, 1980)** reflects the relative volume occupied by aliphatic side chains of non-polar, hydrophobic residues—specifically alanine (A), isoleucine (I), leucine (L), proline (P) and valine (V). In WtpB, 140 of 247 amino acid residues (~57 %) are aliphatic, yielding an AI of 131.94. This elevated value is consistent with the physicochemical properties typical of transmembrane proteins. The high proportion of aliphatic residues likely contributes to the thermal stability of WtpB, enhancing its structural integrity and functional resilience under elevated temperature conditions. The grand average of hydropathy (GRAVY) was calculated as the mean of the hydropathy scores of all amino acid residues (**Gasteiger *et al.*, 2003**). A GRAVY value of 0.854 indicates a predominance of hydrophobic residues in WtpB, consistent with its putative interaction with lipid environments such as membrane and involvement in processes driven by hydrophobic interactions.

Table 1 Global physicochemical characteristics of WtpB from *T. kodakarensis* KOD1, as predicted by ProtParam

Parameter	Calculated Value
Amino acid residues	247
Molecular weight	26840.03 kDa
Positively charged residues (D, E)	21
Negatively charged residues (R, K)	14
Isoelectric point (pI)	9.69
Molar attenuation coefficient (ε) at 280 nm	31400 M^{-1} cm^{-1}
Instability index	27.52
Aliphatic index (AI)	131.94
Grand average of hydropathy index (GRAVY)	0.854

Structural features

The structural features of WtpB are summarized in Table 2. As WtpB from *T. kodakarensis* KOD1 lacks cysteine residues, no disulfide bonds are predicted. FoldIndex (**Prilusky *et al.*, 2005**), which assesses the likelihood of intrinsic disorder, indicates that WtpB is fully ordered, with no disordered residues and a disorder probability of zero. The accessible surface areas of the backbone and side chains are 935.2 Å² and 13,876.7 Å², respectively.

Lower predicted resolution values, particularly below 2.0 Å, indicate higher-quality, well-ordered NMR protein structures with greater structural detail (**Berjanskii *et al.*, 2012**). Mean hydrogen-bond energy is a key indicator of structural validity, reflecting conformational stability and proper folding (**Pace *et al.*, 2012**). The predicted value (-1.8 kJ mol^{-1}) supports a physically plausible WtpB model, with negative energy indicating favourable, stabilizing hydrogen-bond formation. Similarly, the free energy of folding ($\Delta G_{folding}$) is a central determinant of protein stability (**Chong and Ham, 2001**). The predicted value (-220.41 kJ mol^{-1}) indicates an exceptionally stable, well-folded structure consistent with a native state (**Masson and Lushchekina, 2022**). A large predicted solvent-accessible surface area (SASA) indicates a relatively extended protein conformation (**Marsh and Teichmann, 2011**). Consistently, the total volume (32,329.3 Å³) suggests a medium-to-large protein, corresponding to approximately 250–350 residues and aligning with the size of WtpB (247 residues).

Table 2 Structural features of WtpB from *T. kodakarensis* KOD1 predicted using SCRATCH, FoldIndex, VADAR, and ResProx tools

Parameter	Calculated Value
Predicted resolution	1.195 Å
Disordered residues	0
Disorder probability	0 %
Unfoldability	0.447
Total solvent accessible surface area	14811.8 Å²
Total volume (packing)	32329.3 Å³
Disulfide bonds	0
Residues with H-bonds	236 (95 %)
Mean H-bond distance	2.2 Å
Mean H-bond energy	-1.8 kJ mol^{-1}
Residues 95 % buried	48
Free energy of folding	-220.41 kJ mol^{-1}

Structure validation

Structural validation provides a comprehensive assessment of stereochemical quality, aiding in the evaluation of model reliability. The structural quality of WtpB was evaluated using the Ramachandran plot, based on the distribution of backbone torsion angles φ and ψ, calculated via PROCHECK (**Hollingsworth and Karplus, 2010**). As shown in Fig. 4a, 95.5% of residues (211 out of 247) were located within the most favoured regions, indicative of a well-defined structure. An additional 4.1% (9 residues) and 0.4% (1 residue) occupied the additionally allowed and generously allowed regions, respectively, with no residues falling in disallowed regions. A model with over 90% of residues in favoured regions is generally considered of high quality.

Further validation using the ProQ neural network predictor yielded a Levitt–Gerstein (LG) score of 9.228 and a MaxSub score of 0.407, indicative of a highly reliable model (**Levitt and Gerstein, 1998**; **Siew *et al.*, 2000**; **Cristobal *et al.*, 2001**). The QMEAN score of 0.549 with a Z-score of –0.83 (Fig. 4b) is consistent with values reported for experimentally resolved membrane proteins, including ABC permeases, which typically exhibit QMEAN scores in the range of around 0.5–0.7 and Z-scores near zero (**Benkert *et al.*, 2009**; **Waterhouse *et al.*, 2018**). For instance, structurally characterized ABC transporter permeases such as Sav1866 and MsbA display comparable global quality metrics when evaluated against statistical potentials derived from high-resolution structures (**Dawson and Locher, 2006**; **Ward *et al.*, 2007**). MolProbity analysis yielded a score of 0.94, indicating high overall structural quality, as lower scores correspond to better models. The clashscore was 1.28, reflecting the number of serious steric overlaps per 1,000 atoms; lower values similarly indicate improved stereochemical quality (**Williams *et al.*, 2018**). Collectively, these assessments indicate correctness of the WtpB structural model from *T. kodakarensis* KOD1 with comparable quality to experimentally determined ABC permease structures.

Prediction of WtpB-associated proteins

Accessory interacting proteins assist the primary protein in performing its function, or contribute to its proper folding, stabilization, and cellular localization. Ten accessory proteins associated with WtpB in *T. kodakarensis* KOD1 were identified using the STRING database (**Szklarczyk *et al.*, 2023**). The confidence scores of these predicted interactions are shown in Fig. 5. Notably, WtpA (a periplasmic component) and WtpC (an ATPase component) exhibit the strongest associations with WtpB, with confidence scores of 0.992 and 0.991, respectively. Together, WtpA, WtpB, and WtpC form the ABC transporter complex WtpABC, which is implicated in molybdate/tungstate transport.

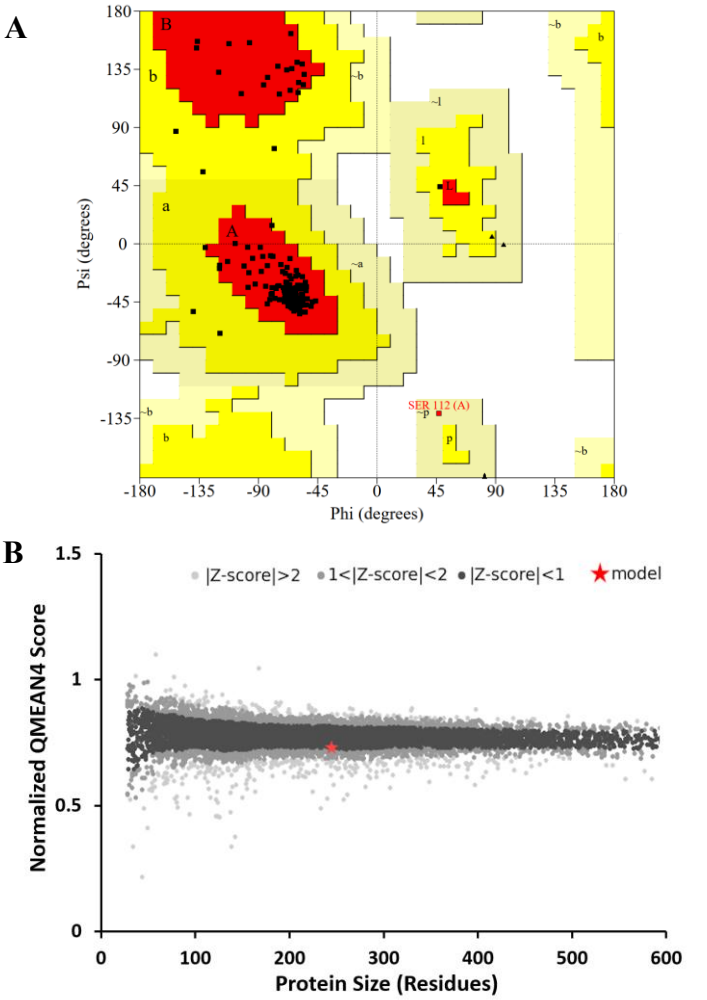

Figure 4 Validation of the WtpB structural model. (A) Ramachandran plot generated by PROCHECK, showing the distribution of backbone dihedral angles and the absence of residues in disallowed regions. (B) QMEAN quality assessment of the WtpB model. The normalized QMEAN score (y-axis) is compared against a reference set of high-resolution, non-redundant Protein Data Bank (PDB) structures, indicating the overall reliability of the model.

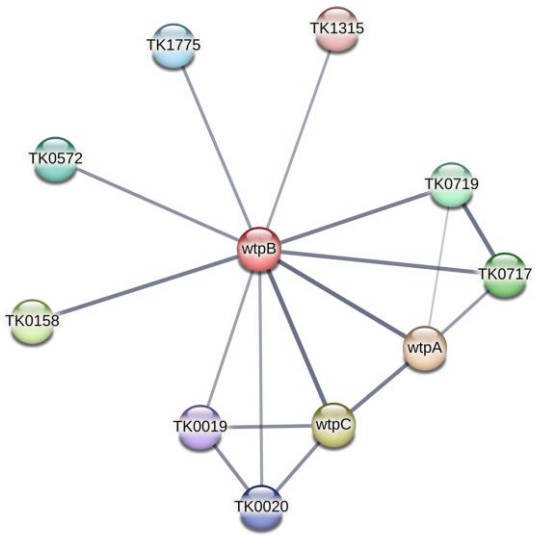

Figure 5 Confidence map of ten accessory proteins functionally associated with WtpB, implicated in molybdate/tungstate transport in *T. kodakarensis* KOD1. Protein–protein interaction network was generated using STRING.

Phylogenetic analysis

Figure 6 illustrates the phylogenetic relationships among WtpB from *T. kodakarensis* KOD1 and homologous molybdate/tungstate transport system permease proteins across 30 *Thermococcus* species. The percentage of replicate trees in which the associated taxa clustered together in the bootstrap test (1000 replicates) are shown next to the branches (**Felsenstein, 1985**). Closely related taxa, including *T. archaeon*, *T. peptonophilus*, and *T. stetteri* are obligate anaerobes inhabiting deep-sea hydrothermal vents, and typically employ elemental sulfur as a terminal electron acceptor (**Miroshnichenko *et al*., 1989; González *et al*., 1995**). These species share high sequence identity with WtpB of *T. kodakarensis*, ranging from 93.5 % to 97.1 %. In contrast, WtpB from *Pyrococcus furiosus*, a hyperthermophilic model archaeon (**Bevers *et al*., 2006**), displays only 72.6 % identity and was used as an outgroup. The phylogenetic tree resolves six additional clusters, with *T. Barophilus* (hyperpiezophile), *T. gammatolerans* (radioresistant), and *T. litoralis* (thermozyme-producing) among the most prominent representatives, showing 75.0–86.4 % sequence identity to *T. kodakarensis* WtpB.

Table 3 Predicted functional partners of WtpB in *T. kodakarensis* KOD1 as identified by STRING analysis. Node identifiers correspond to those shown in Fig. 4. Interactions are based on STRING confidence scores, with only high-confidence associations included.

Node	Description	Confidence Score
WtpA	ABC-type molybdate transport system, periplasmic component	0.992
WtpC	ABC-type sulfate transport system, ATPase component	0.991
TK0158	ABC-type iron (III) transport system, ATPase component	0.911
TK0717	ABC-type molybdate transport system, periplasmic component	0.894
TK0719	ABC-type molybdate transport system, ATPase component	0.892
TK0572	ABC-type iron (III) transport system, ATPase component	0.763
TK1775	ABC-type maltdextrin transport system, ATPase component	0.710
TK0020	Hypothetical protein, conserved	0.661
TK0019	Predicted ABC-type transport system, ATPase component	0.660
TK1315	3′-phosphoadenosine 5′ -phosphosulfate reductase	0.636

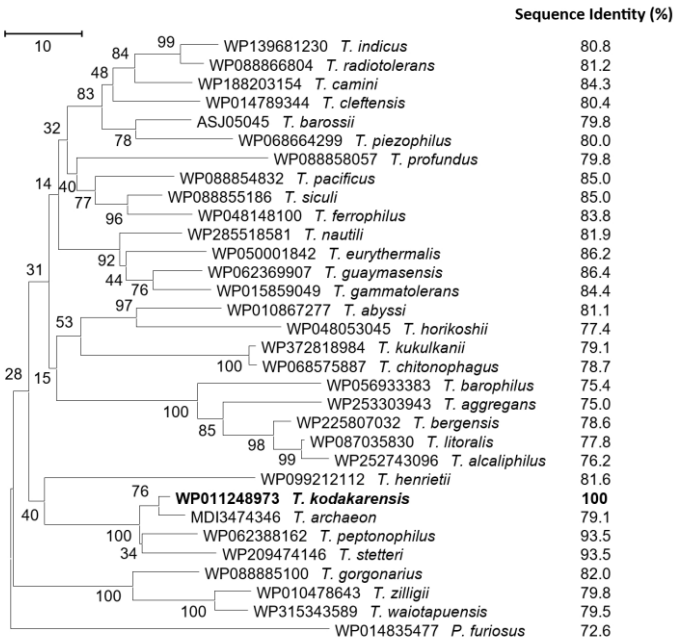

Figure 6 Consensus phylogenetic tree of WtpB homologues from selected *Thermococcus* species. Accession numbers are provided for each sequence. WtpB from *Pyrococcus furiosus* (WP014835477) was used as an outgroup. The tree is drawn to scale, with branch lengths representing the number of amino acid substitutions per site. Evolutionary analysis was performed using MEGA12.

CONCLUSION

This study provides a structural and functional analysis of WtpB from *T. kodakarensis* KOD1, highlighting its role in the molybdate/tungstate ABC transporter system. The protein exhibits a conserved α-helical architecture with distinct functional regions, including PBP-binding loops, a gate region, and an ABC-ATPase interface, supporting its involvement in energy-coupled metal oxyanion uptake. Physicochemical properties indicate thermal stability and hydrophobicity consistent with membrane association in a hyperthermophilic

archaeon. Structural validation and interaction analyses support a biologically plausible model in which WtpB associates with WtpA and WtpC. Phylogenetic analysis further indicates strong evolutionary conservation among *Thermococcus* species. Collectively, these results provide a molecular basis for selective oxyanion transport and support further mechanistic and applied studies of archaeal transporter systems.

While these findings collectively provide meaningful structural and functional insights, it should be recognized that they are derived from computational and predictive analyses; therefore, the proposed structural features, functional site assignments, and protein–protein interaction partners should be interpreted as testable hypotheses rather than experimentally validated mechanisms. Future work employing site-directed mutagenesis, ligand-binding assays, cross-linking studies, and cryo-electron microscopy or X-ray crystallography, along with molecular dynamics simulations, will be essential to experimentally confirm the structural dynamics, interaction interfaces, and transport mechanism of WtpB within the WtpABC system.

REFERENCES

Altschul, S. F., Madden, T. L., Schäffer, A. A., Zhang, J., Zhang, Z., Miller, W., & Lipman, D. J. (1997). Gapped BLAST and PSI-BLAST: a new generation of protein database search programs. *Nucleic Acids Research*, *25*, 3389-3402. https://doi.org/10.1093/nar/25.17.3389

Benkert, P., Künzli, M., & Schwede, T. (2009). QMEAN server for protein model quality estimation. *Nucleic Acids Research*, *37*, W510-W514. http://doi.org/10.1128/EC.4.3.625-632.2005

Berjanskii, M., Zhou, J., Liang, Y., Lin, G., & Wishart, D. S. (2012). Resolution-by-proxy: a simple measure for assessing and comparing the overall quality of NMR protein structures. *Journal of Biomolecular NMR*, *53*(3), 167-180. http://doi.org/10.1107/s10858-012-9637-2

Bevers, L. E., Hagedoorn, P. L., Krijger, G. C., & Hagen, W. R. (2006). Tungsten transport protein A (WtpA) in *Pyrococcus furiosus*: the first member of a new class of tungstate and molybdate transporters. *Journal of Bacteriology*, *188*(18), 6498-6505. https://doi.org/10.1128/JB.00548-06

Bevers, L. E., Schwarz, G., & Hagen, W. R. (2011). A molecular basis for tungstate selectivity in prokaryotic ABC transport systems. *Journal of Bacteriology*, *193*(18), 4999-5001. https://doi.org/10.1128/JB.05056

Cheng, J., Randall, A. Z., Sweredoski, M. J., & Baldi, P. (2005). SCRATCH: a protein structure and structural feature prediction server. *Nucleic Acids Res*earch, *33*, W72-W76. http://dx.doi.org/10.1093/nar/gki396

Chong, S. H., & Ham, S. (2001). Protein folding thermodynamics: A new approach. The Journal of Physical Chemistry B, 118(19), 5017-5025. https://doi.org/10.1021/jp500269m

Cristobal, S., Zemla, A., Fischer, D., Rychlewski, L., & Elofsson, A. (2001). A study of quality measures for protein threading models. *BMC Bioinformatics*, *2*(1), 5. http://doi.org/10.1186/1471-2105-2-5

Dawson, R. J. P., & Locher, K. P. (2006). Structure of a bacterial multidrug ABC transporter. *Nature*, *443*(7108), 180–185. http://doi.org/10.1038/nature05155

Drozdetskiy, A., Cole, C., Procter, J., Barton, G. J. (2015). JPred4: a protein secondary structure prediction server. *Nucleic Acids Research*, *43*(W1), W389-394. http://doi.org/10.1093/nar/gkv332

Felsenstein, J. (1985). Confidence limits on phylogenies: An approach using the bootstrap. *Evolution*, *39*(4), 783-791. https://doi.org/10.2307/2408678

Fukui, T., Atomi H., Kanai, T., Matsumi, R., Fujiwara, S., & Imanaka, T. (2005). Complete genome sequence of the hyperthermophilic archaeon *Thermococcus kodakaraensis* KOD1 and comparison with *Pyrococcus* genomes. *Genome Research*, *15*(3), 352-363. http://doi.org/10.1101/gr.3003105

Gasteiger, E., Gattiker, A., Hoogland, C., Ivanyi, I., Appel, R. D., & Bairoch, A. (2003). ExPASy: the proteomics server for in-depth protein knowledge and analysis. *Nucleic Acids Research*, *31*, 3784-3788. https://www.ncbi.nlm.nih.gov/pubmed/12824418

Gerber, S., Comellas-Bigler, M., Goetz, B. A., & Locher, K. P. (2008). Structural basis of trans-inhibition in a molybdate/tungstate ABC transporter. *Science*, *321*(5886), 246-250. https://doi.org/10.1126/science.1156213

González J. M., Kato, C., & Horikoshi, K. (1995). *Thermococcus peptonophilus* sp. nov., a fast-growing, extremely thermophilic archaebacterium isolated from deep-sea hydrothermal vents. *Archives of Microbiology*, *164*(3), 159-164. https://doi.org/10.1007/s002030050249

Guruprasad, K., Reddy, B. V., & Pandit, M. W. (1990). Correlation between stability of a protein and its dipeptide composition: a novel approach for predicting *in vivo* stability of a protein from its primary sequence. *Protein Engineering*, *4*(2), 155-161. http://doi.org/10.1093/protein/4.2.155

Hall, T.A. (1999). BioEdit: A user-friendly biological sequence alignment editor and analysis program for Windows 95/98/NT. *Nucleic Acids Symposium Series*, *41*, 95-98.

Hetzer, A., Morgan, H. W., McDonald, I. R., & Daughney, C. J. (2007). Microbial life in champagne pool, a geothermal spring in Waiotapu, New Zealand. *Extremophiles*, *11* (4), 605-614. http://doi.org/10.1007/s00792-007-0073-2

Hollingsworth, S. A., & Karplus, P. A. (2010). A fresh look at the Ramachandran plot and the occurrence of standard structures in proteins. *Biomolecular Concepts*, *1*(3-4), 271-283. http://doi.org/10.1515/BMC.2010.022

Hsin, J., Arkhipov, A., Yin, Y., Stone, J. E., & Schulten, K. (2008). Using VMD: an introductory tutorial. *Current Protocols in Bioinformatics*, *5*, 5.7. http://doi.org/10.1002/0471250953.bi0507s24

Ikai, A. (1980). Thermostability and aliphatic index of globular proteins. *Journal of Biochemistry*, *88*, 1895-1898. http://doi.org/10.1093/oxfordjournals.jbchem.a133168

Kazakov, A. E., Rajeev, L., Luning, E. G., Zane, G. M., Siddartha, K., Rodionov, D. A., …, & Novichkov, P. S. (2013). New family of tungstate-responsive transcriptional regulators in sulfate-reducing bacteria. *Journal of Bacteriology*, *195*(19), 4466-4475. https://doi.org/10.1128/JB.00679-13

Krupovic, M., Gonnet, M., Hania, W. B., Forterre, P., Erauso, G. (2013). Insights into dynamics of mobile genetic elements in hyperthermophilic environments from five new *Thermococcus* plasmids. *PLOS One*, *8*(1), e49044. http://doi.org/10.1371/journal.pone.0049044

Kumar, S., Stecher, G., Suleski, M., Sanderford, M., Sharma, S., & Tamura, K. (2024). MEGA12: Molecular evolutionary genetic analysis version 12 for adaptive and green computing. *Molecular Biology and Evolution*, *41*(12), msae263. http://doi.org/ 10.1093/molbev/msae263

Larkin, M. A., Blackshields, G., Brown, N. P., Chenna, R., Mcgettigan, P. A., Mcwilliam, H., ... & Higgins, D. G. (2007). Clustal W and Clustal X version 2.0. *Bioinformatics*, *23*, 2947-2948. http://doi.org/10.1093/bioinformatics/btm404

Laskowski, R. A., Macarthur, M. W., Moss, D. S., & Thornton, J.M. (1993). PROCHECK - a program to check the stereochemical quality of protein structures. *Journal of Applied Crystallography*, *26*, 283-291. http://doi.org/10.1107/S0021889892009944

Levitt, M., & Gerstein, M. (1998). A unified statistical framework for sequence comparison and structure comparison. *Proceedings of National Academy of Sciences of the USA*, *95*(11), 5913-5920. http://doi.org/10.1073/pnas.95.11.5913

Marsh, J.A., & Teichmann, S. A. (2011). Relative solvent accessible surface area predicts protein conformational changes upon binding. *Structure*, *19*(6), 859-867. http://doi.org/10.1016/j.str.2011.03.010

Masson, P., & Lushchekina, S. (2022). Conformational stability and denaturation processes of proteins investigated by electrophoresis under extreme conditions. *Molecules*, *27*(20), 6861. http://doi.org/10.3390/molecules27206861

Mendel, R. R., & Kruse, T. (2012). Cell biology of molybdenum in plants and humans. *Biochimica et Biophysica Acta (BBA)-Molecular Cell Research*, *1823*(9), 1568-1579. https://doi.org/10.1016/j.bbamcr.2012.02.007

Miroshnichenko, M. L., Bonch-Osmolovskaya, E. A., Neuner, A., Kostrikina, N. A., Chernych, N. A., Alekseev, V. A. (1989). *Thermococcus stetteri* sp. nov., a new extremely thermophilic marine sulfur-metabolizing archaebacterium. *Systematic and Applied Microbiology*, *12*(3), 257-262. https://doi.org/10.1016/S0723-2020(89)80071-2

Mourez, M., Hofnung, M., & Dassa, E. (1997). Subunit interactions in ABC transporters: a conserved sequence in hydrophobic membrane proteins of periplasmic permeases defines an important site of interaction with the ATPase subunits. *EMBO Journal*, *16*, 3066-3077. https://doi.org/10.1093/emboj/16.11.3066

Moustakas, M. (2021). The role of metal ions in biology, biochemistry and medicine. *Materials (Basel)*, *14*(3), 549. http://doi.org/10.3390/ma14030549

Nie, M., & Kumar, S. (2000). Molecular Evolution and Phylogenetics. Oxford University Press, New York. https://doi.org/10.1017/S0016672301219405

Nishioka, M., Mizuguchi, H., Fujiwara, S., Komatsubara, S., Kitabayashi, M., Uemura, H., …, & Imanaka, T. (2001). Long and accurate PCR with a mixture of KOD DNA polymerase and its exonuclease deficient mutant enzyme. *Journal of Biotechnology*, *88*(2), 141-149. http://doi.org/10.1016/s0168-1656(01)00275-9

Pace, C. N., Fu, H., Lee Fryar, K., Landua, J., Trevino, S. R., Schell, D., ..., & Grimsley, G. R. (2014). Contribution of hydrogen bonds to protein stability. *Protein Science*, *23*(5), 652-661. http://doi.org/10.1002/pro.2449

Prilusky, J., Felder, C. E., Zeev-Ben-Mordehai, T., Rydberg, E. H., Man, O., Beckmann, J. S., ..., & Sussman, J. L. (2005). FoldIndex: a simple tool to predict whether a given protein sequence is intrinsically unfolded. *Bioinformatics*, *21*(16), 3435-3438. http://doi.org/10.1093/bioinformatics/bti537

Saito, N., & Nei, M. (1987). The neighbor-joining method: a new method for reconstructing phylogenetic trees. *Molecular Biology and Evolution*, *4*, 406-425. http://doi.org/10.1093/oxfordjournals.molbev.a040454

Siew, N., Elofsson, A., Rychlewski, L., & Fischer, D. (2000). MaxSub: an automated measure for the assessment of protein structure prediction quality. *Bioinformatics*, *16*(9), 776-785. http://doi.org/10.1093/bioinformatics/16.9.776

Szklarczyk, D., Kirsch, R., Koutrouli, M., Nastou, K., Mehryary, F., Hachilif, R., …, & von Mering, C. (2023). The STRING database in 2023: protein–protein association networks and functional enrichment analyses for any sequenced genome of interest. *Nucleic Acids Res*earch, *51*(D1), D638-D346. http://doi.org/10.1093/nar/gkac1000

Wallner, B., & Elofsson, A. (2003). Can correct protein models be identified? *Protein Sci*ence, *12*(5), 1073-1086. http://doi.org/10.1110/ps.0236803

Wang, J., Chitsaz, F., Derbyshire, M. K., Gonzales, N. R., Gwadz, M., Lu, S., ..., & Marchler-Bauer, A. (2023). The conserved domain database in 2023. *Nucleic Acids Research*, *51*(D1), D384-D388. http://doi.org/10.1093/nar/gkac1096

Ward, A., Reyes, C. L., Yu, J., Roth, C. B., & Chang, G. (2007). Flexibility in the ABC transporter MsbA: Alternating access with a twist. *Proceedings of the National Academy of Sciences USA*, *104*(48), 19005–19010. http://doi.org/10.1073/pnas.0709388104

Waterhouse, A., Bertoni, M., Bienert, S., Studer, G., Tauriello, G., Gumienny, R., …, & Schwede, T. (2018). SWISS-MODEL: Homology modelling of protein structures and complexes. *Nucleic Acids Research*, *46*(W1), W296–W303. http://doi.org/10.1093/nar/gky427

Wheaton, G. H., Mukherjee, A., Kelly, R. M. (2016). Transcriptomes of the extremely thermoacidophilic archaeon *Metallosphaera sedula* exposed to metal "shock" reveal generic and specific metal responses. *Applied and Environmental Microbiology*, *82*(15), 4613-4627. https://doi.org/10.1128/AEM.01176-16

Willard, L., Ranjan, A., Zhang, H., Monzavi, H., Boyko, R. F., Sykes, B. D., & Wishart, D. S. (2003). VADAR: a web server for quantitative evaluation of protein structure quality. *Nucleic Acids Research*, *31*(13), 3316-3319. http://doi.org/10.1093/nar/gkg565

Williams, C. J., Headd, J. J., Moriarty, N. W., Prisant, M. G., Videau, L. L., Deis, L. N., …, & Richardson D. C. (2018). MolProbity: More and better reference data for improved all-atom structure validation. *Protein Science*, *27*(1), 293-315. http://doi.org/10.1002/pro.3330

Winiarska, A., Ramírez-Amador, F., Hege, D., Gemmecker, Y., Prinz, S., Hochberg, G., …, & Schuller, J. M. (2023) A bacterial tungsten-containing aldehyde oxidoreductase forms an enzymatic decorated protein nanowire. *Science Advances*, *9*(22), eadg6689. https://doi.org/10.1126/sciadv.adg6689